Regular Article

PHYSICAL CHEMISTRY RESEARCH
Published by the
Iranian Chemical Society
www.physchemres.org
info@physchemres.org

***Phys. Chem. Res.**, Vol. 1, No. 2, 152-165, December 2013.*

Molecular Dynamics Studies on the Denaturation of Polyalanine in the Presence of Guanidinium Chloride at Low Concentration

D. Ajloo*, S. Ghalehaghababaie and N. Mahmoodabadi
School of Chemistry, Damghan University, Damghan, Iran
(Received 26 March 2013, Accepted 22 August 2013)

Molecular dynamic simulation is a powerful method that monitors all variations in the atomic level in explicit solvent. By this method we can calculate many chemical and biochemical properties of large scale biological systems. In this work, all-atom molecular dynamic simulation of polyalanine (PA) was investigated in the presence of 0.224, 0.448, 0.673, 0.897 and 1.122 M of guanidinium chloride (GdmCl) at 273-395 K by molecular dynamics simulation. Analysis of surface area, radial distribution function, radius of gyration, heat capacity, hydrogen bond, helix, coil and beta contents showed that an intermediate appears on the way of helix to coil transition. GdmCl at low concentration increases the midpoint of transition temperature (T_m), number of solvent molecules in the hydration layer and interapeptide hydrogen bond as well as decreases in rate of helix to coil transition. Thus, the role of guanidine at low concentration is as the same as osmolytes which decreases the beta form and, increases hydration layer and the polypeptide thermal stability.

Keywords: Phase transition, Polyalanine, Thermal stability, Heat capacity, Intermediate

INTRODUCTION

Polyalanine (PA) peptide has important biological effects, and can cause various human illnesses and neurodegenerative diseases [1]. Detailed structural investigation of PA peptide is important to identify their conformational properties, which can help in understanding the mechanisms underlying these human illnesses and neurodegenerative diseases. Several experimental and theoretical studies have been performed so far to examine the structural features of PA peptide and their derivatives [2]. However, determination of the conformational properties of PA in experimental methods, is a challenging task, because it is quite insoluble in water, and this insolubility leads to the aggregation of these PAs.

Peptide model systems have been useful in studies of fibril aggregate formation. The aggregation observed in protein conformational diseases is the outcome of significant new β-sheet structure not present in the native state. Changes in sequence or shape of a protein may lead to a conformational disease. Conformational diseases are typically expressed in the appearance of amyloid fibrils. Understanding amyloid seed formation and elongation at the molecular level presents a major challenge, as it may lead to novel approaches in design and therapy [3]. Short peptide systems are considerably simpler than those of large proteins, and obtaining atomic detail on peptide amyloid formation from X-ray diffraction of amyloid fibrils has proved to be difficult. Furthermore, current experimental methodologies encounter difficulties in obtaining atomic details regarding seed formation and propagation. Knowledge about mechanism of misfolding or monitoring transition state and intermediate increase capability of designing drug for treatment of diseases [4]. Since the experimental methods are expensive, computational methods such as molecular dynamic [5] and QSAR [6,7] can facilitate drug design.

It has been proved that osmolystes can inhibit the protein aggregation and are effective in Alzheimer treatment. Based on these experimental results, Liu and coworkers have simulated inhibition properties of trehalose (an osmolyte) on the aggregation of amyloid by molecular dynamics method [5]. On the other hand, structure-function relationship is a known correlation so that it needs to understand the protein structural changes. The structural changes may occur by thermal and chemical denaturants

*Corresponding author. E-mail: ajloo@du.ac.ir

[8,9] which can be studied by different methods and techniques [10-15].

One of the most studied structural changes is the helix to coil phase transition in polypeptides. Experimentally, extensive studies of the helix-coil transition in polypeptides have been conducted [16]. The dependence of the heat capacity and helicity of the polypeptide on temperature was measured using differential scanning calorimetry and circular dichroism methods [17], while the kinetic of the helix-coil transition of the 21-residue alanine polypeptide was investigated by means of infrared spectroscopy [18-20].

Alternately, it was reported that chemical species also induce structural changes to proteins. Several experimental evidences have been collected regarding to the effects of solutes that may act either as a stabilizing agent or as a denaturing agent. For instance, ethylene glycol [21], some salts [22], sugars and polyols [23] are known to stabilize proteins in aqueous solutions, whereas guanidine hydrochloride [24], urea [25] and surfactant [8] act as denaturing agents.

Guanidine cation is the most powerful protein denaturant commonly used to study the protein stability and folding [26,27], despite the fact that the detailed mechanism of its denaturation properties remains unresolved. Gdm ions bind to polypeptides, and this binding is expected to provide a significant contribution to the protein denaturation, because on unfolding, many hydrogen-bonded of amides in buried backbone become more available for binding of denaturant. In contrast, the effect of denaturants on increasing the aqueous solubility of hydrophobic side chains exposed on unfolding has been rationalized in terms of an effect on the hydrogen-bond network of water.

Gdm+ ions are ‘‘sticky’’ in the manner described by Collins [28] for the ‘‘pushing’’of weakly hydrated ions (chaotropes) onto weakly hydrated surfaces by relatively stronger water-water interactions. Denaturation results to a greater or less extent from the favorable interaction with the polypeptide backbone exposed on unfolding as described for Gdm and urea [29]. In contrast, a large class of sugars and other polyols (osmolytes), which stabilize proteins, interacts unfavorably with the peptide backbone and is preferentially excluded from the protein surface [30]. The differences in the secondary structure preferences for several residues, which show α-helical preferences in the urea-denatured state and β-preferences in the guanidine-denatured state, may be attributed to the differences in the perturbations caused by these denaturants at these sites [31].

Guanidinium hydrochloride (GdmCl) at low concentrations significantly stabilizes the Fyn SH3 domain [32]. Stabilizing effect is manifested through a dramatic decrease in the unfolding rate of the domain with the folding rate being affected to the lowest extend. This behavior is in contrast to the effect of NaCl, which stabilizes this domain by accelerating the folding rate. This implies that the stabilizing effect of GdmCl is not predominantly ionic in nature. It was suggested those many proteins that normally interact with arginine-containing ligands may also be able to specifically interact with guanidinium ion. Thus, some caution should be used when using GdmCl as a denaturant in protein folding studies [32].

The effects of GdmCl on protein stability are particularly complicated due to its ionic character. Ions can either bind to the folded or unfolded states of proteins or influence stability through “screening” columbic interactions, the Hofmeister effect, or changing the structure of the solvent [33,34]. Although GdmCl is thought of primarily as a denaturant, there are many reported cases that show low concentrations of GdmCl actually stabilize proteins [35-38]. In the majority of these cases, it has been shown that the ionic nature of GdmCl is the main factor in its stabilizing effect [36,37]. However, some studies have suggested that GdmCl may cause protein stabilization in a more specific manner [35].

In this paper, we use the MD approach to study the α-helix ↔ random coil phase transition in alanine polypeptides in different temperatures in the presence of GdmCl at low concentration. The structural changes are monitored by variation in helix, coil and beta content. Distribution of water and ions in the protein surrounding is followed by radial distribution function. Protein stability and intermediate monitoring are investigated by variation of heat capacity in different temperatures and GdmCl concentrations.

Simulation Details

Initial helix structure of polyalanine was created by Hyperchem 7.0 (Scheme 1). The N and C termini of polyalanine are capped, respectively, by neutral acetyl and

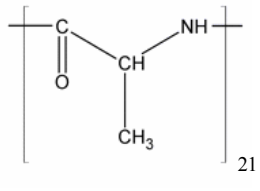

(a)

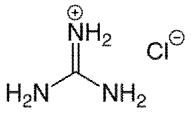

(b)

Scheme 1. Structure of a) polyalanine and b) guanidine chloride

amine groups, and the simulated sequence is 21 Ala. Force field parameters and the topology for the guanidinium chloride molecule were generated using the PRODRG2 server (http://davapc1.bioch.dundee.ac.uk/cgi bin/prodrg_ beta) [39]. The peptide was first placed in a cubic box with periodic boundary conditions. The size of the cubic box throughout the simulations was 70 nm^3 with negligible volume fluctuations, where the distance between the peptide and the box edges was chosen to be about 1 nm. This allows us to rule out any unwanted effects [40], which may arise from the applied periodic boundary conditions.

Finally, non-overlapping water molecules and Cl ions were randomly added into the simulation box (Table 1).

Initial configurations were minimized in three steps; minimization of peptide energy, minimization of ions and water molecules (position restraint), minimization of whole of system. After 400 steps of energy minimization, the system was equilibrated for 0.8 ns at constant pressure (1 atm) and temperatures (273-390 K).

Here, we consider high-temperature molecular dynamics as an approach for generating conformations. The use of high temperatures provides the required energy to surmount energetic barriers so that many adjacent local minima can be explored. Comparison of the results related to the high temperature molecular dynamics with a direct conformational search method, [41,42] showed that the two methods did not overlap much in conformational space. Simple geometric measures of the conformational space indicated that the direct method covers more space than that of molecular dynamics at the lower temperature, but not at 1500 K. The results suggest that high-temperature molecular dynamics can aid in conformational searches. Although such high temperatures are not physically meaningful, they are of interest for exploring conformational space. High-temperature molecular dynamics is a reasonable conformational search method when it is restricted to peptide segments on the order of a dozen residues and perhaps morefor a cyclic system. This range is usually considered in MD simulation.

All MD simulations were carried out using the GROMACS 3.3 package [43] along with the GROMOS96 force field [44]. The simple point charge (SPC) model was

Table 1. Number of Guanidine and Chloride Ions and Number of Water Molecules in the Molecular Dynamics Box

Guanidine concentration (M)	Number of guanidine ions	Number of water molecules	Number of chloride ions
0	0	2296	0
0.224	10	2279	10
0.448	20	2265	20
0.672	30	2252	30
0.896	40	2241	40
1.122	50	2228	50

used to describe water [45]. A 2 fs time step was used to integrate the equations of motion with the Verlet algorithm [46]. The total simulation time of the runs were 20 ns. The long-range electrostatic interactions were treated with the particle mesh Ewald method [47]. A non bond pair list cutoff of 0.9 nm was used, and the nstlist was updated every ten steps. The LINCS algorithm was used to constrain all bond lengths [48].

Temperatures (273-390 K) and pressure (1 atm) were controlled by the Nose-Hoover thermostat [49, 50] and Parrinello-Rahman barostate [51] with coupling constants of 0.1 and 0.5, respectively. For all simulations, the atomic coordinates were saved every 50 ps for analysis. MD simulations were run on a 40-CPU clustered Rocks network. All calculation were done three times and the consistent results were obtained (Fig. S1)

Analyses

The simulation trajectories were analyzed using several auxiliary programs provided with the GROMACS 3.3 package. The "g_helix" key computes all kinds of helix properties. In addition, the helix, coil, and beta content were calculated using VADAR [52]. The "g_rms" evaluates the deviation of the structure from the original starting structure over the course of the simulation. RMSD of certain atoms in a molecule with respect to a reference structure can be calculated as following:

$$RMSD(t_1,t_2)=\left[\frac{1}{M}\sum_{i=1}^{N}m_i\|r_i(t_2)-r_i(t_1)\|^2\right]^{1/2} \quad (1)$$

Where m_i is the mass of atom i and r_i the position of atom i with respect to the center of mass of the molecule. The RMSD can be computed of the backbone or of the whole protein. The "g_hbond" calculates the hydrogen bond interactions between hydrogen donors and acceptors through the course of the simulation. Hydrogen bonds are considered to be intact if the donor-to-acceptor distance is less than 0.35 nm and the donor-hydrogen-acceptor angle is within 30° of linearity. The "g_rdf" calculates radial distribution functions in different ways. The normal method is around a (set of) particle(s), the other method is around the center of mass of a set of particles. In this study the center of mass of molecules was considered. The radial distribution function (RDF) or pair correlation function $g_{AB}(r)$ between particles of type A and B is defined in the following way:

$$g_{AB}(r)=\frac{\langle\rho_B(r)\rangle}{\langle\rho_B\rangle_{local}} \quad (2)$$

where $<\rho_B(r)>$ is the particle density of type B at the distance r around particles A and, $<\rho_B>_{local}$ is the particle density of type B averaged over all spheres around particles A with radius r_{max}. Usually, the value of r_{max} is considered as the half of the box length. The "g_gyrate" measures the radius of gyration. This quantity gives a measure of the "compactness" of the structure. This gives a measure of the mass of the atom(s) relative to the center of the mass of the molecule and is calculated as follow:

$$R_g=\left(\frac{\sum_i m_i\|r_i\|^2}{\sum_i m_i}\right)^{\frac{1}{2}} \quad (3)$$

Where m_i is the mass of atom i and r_i is the position of atom i with respect to the center of mass of the molecule. The "g_sas" calculates the peptide accessible surface for the solvent molecules. We have considered the polypeptide in the NPT ensemble and calculated the heat capacity of the system using fluctuation theorem [20]:

$$C_p=\frac{\langle H^2\rangle-\langle H\rangle^2}{RT^2} \quad (4)$$

$$\langle H\rangle=\frac{\sum_V\sum_j H_i e^{-E_{Vj}/kT}e^{-pV/kT}}{\sum_V\sum_j e^{-E_{Vj}/kT}e^{-pV/kT}} \quad (5)$$

$\langle H\rangle$ is the time-averaged value of the polypeptide enthalpy, H_i is the enthalpy of the ith state, and k is the Bolzmann factor. The summation in equation [5] is performed over all accessible states of the system. The average total configurational energies $E + PV$, shown in equation $H = E + PV$, were directly obtained from GROMACS during the simulation.

RESULTS AND DISCUSSION

Time Evolution

The variation of polyalanine structure at different concentration of guanidinium chloride and different temperatures during the 20 ns calculation was investigated. Molecular snapshot of guanidine and chloride ions distribution around polyalanine is shown in Fig. 1.

The Fig. 1 shows that the guanidine chloride denatures polypeptide, so that at the initial time of simulation, polypeptide is unfolded, helix percent decreases and coil increases. At the middle time, the beta structure increases and finally the coil percent increases. At higher temperatures, all helix structure is converted to coil. The discussion of Fig. 2 also supports this issue.

The denaturants affect on the polypeptide structure in two manners a) direct or specific interaction b) indirect or unspecific interaction (effect on solvent distribution). Snapshots of Fig. 1 mostly show unspecific interactions, as discussed in other parts of manuscript. Salting in reagents such as urea and guanidine pull the water from protein adjacent and increases the salvation of polypeptide and unfold it, while salting out reagents push the water around the polypeptide and so increases the folding.

To prevent complexity, water molecules are not shown. Figure 2 shows the time evolution of structural parameters such as hydrophobic, hydrophilic and total solvent accessible surface (SAS), polyalanine intramolecular hydrogen bond (HB-p-p), intermolecular hydrogen bond between polyalanine and solvent (HB-p-sol), radius of gyration (R_g), root mean square deviation from carbon alpha (RMSD), percents of helix, beta and coil.

The variation of hydrophobic SAS shows a decreasing trend to 8500 ps, then, a maximum in the range of 8500 to 16500 ps (dashed rectangle) and finally a smooth trend until 20000 ps. Variation of hydrophilic surface increases up to 3000 ps then decreases to final time. Total surface is similar to hydrophobic surface. It seems that hydrophilic groups become more exposed to the solvent, while the hydrophobics tend to be located in interior of polypeptide.

HB-p-sol shows an increasing trend up to 4500 ps then decreases to final time. Trend of R_g is inverse of RMSD and is similar to the total surface and HB-p-p. It means, at the initial times the interaction of protein with solvent increases and protein-protein decreases.

More significant matter is the presence of a peak in the 10000 to 15000 ps time interval which will be discussed in the next sections.

Temperature Effect

Middle column of Fig. 2 represents temperature effect on the average of variables (last 2 ns) cited in previous section. As a matter of fact, the temperature is a denaturating factor and its enhancing is usually parallel to unfolding of polypeptide. It causes a regular structure or helix convert to an irregular structure or random coil. Increasing the temperature weakens the hydrogen bond, electrostatic and hydrophobic interactions and increases the accessible surface area and polypeptide size. Additionally, in the middle column of Fig. 2, hydrophobic and total surface area, radius of gyration and intramolecular hydrogen bond decreases by temperature while the hydrophilic surface area, RMSD, coil% and beta% increases. It seems that at the first stage, the helix structure is changed and partial unfolding is observed. In this case, some of the unfolded and exposed amino acids interact with each other and form beta structure and new helix structure. Thus, decreasing the surface may be due to the beta and helix formation so that this phenomenon inhibits the perfect unfolding. Helix conformation is as the same as cylindrical form and unfolding phenomenon causes the helix to convert to the random coil or beta which has lower radius of gyration.

Effect of Guanidine Chloride

Last column of Fig. 2 represents the effect of guanidine at low concentration on the cited physical parameters. Hydrophobic and total SAS increases have similar trends. Hydrophilic surface, polypeptide solvent hydrogen bond (HB-pro-sol), R_g and Helix% have inverse trend relative to hydrophobic surface, interamolecular hydrogen bond (HB-pro-pro), RMSD and coil%, respectively.

Molecular Interactions Monitoring

Into clarify these phenomena in the molecular aspect, the snapshot of the process was sampled in different time scales. Figures. 3a-d show that the polypeptide is mostly helix at the initial times, so that helix and coil percent are

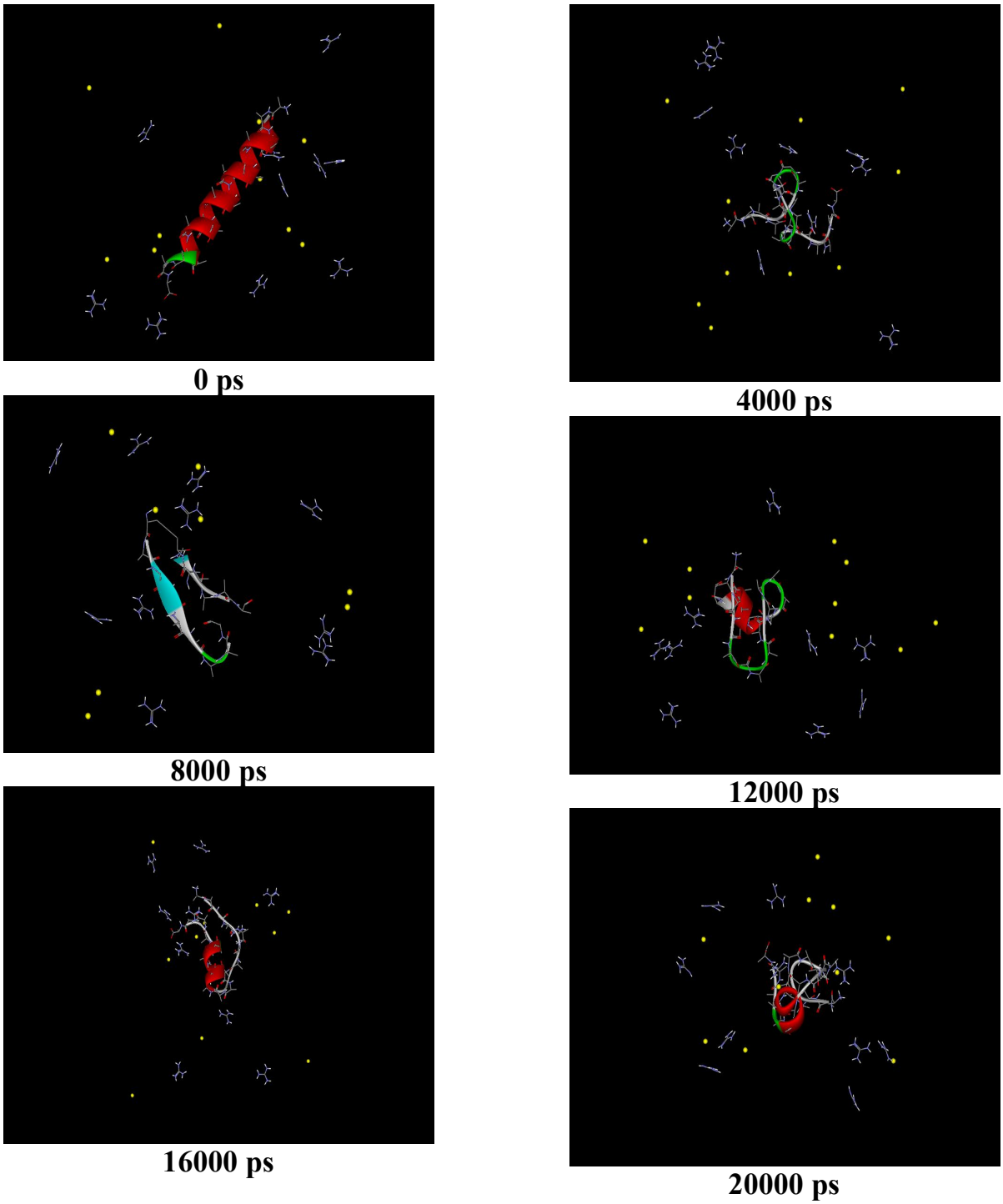

Fig. 1. Molecular snapshot of 10 molecular ions of guanidine chloride around polyalanine at 345 K. Red ribbons, blue, green, and white bands represent helical structure, beta sheet, turn and coil structure, respectively. Chloride ions were shown by yellow dot.

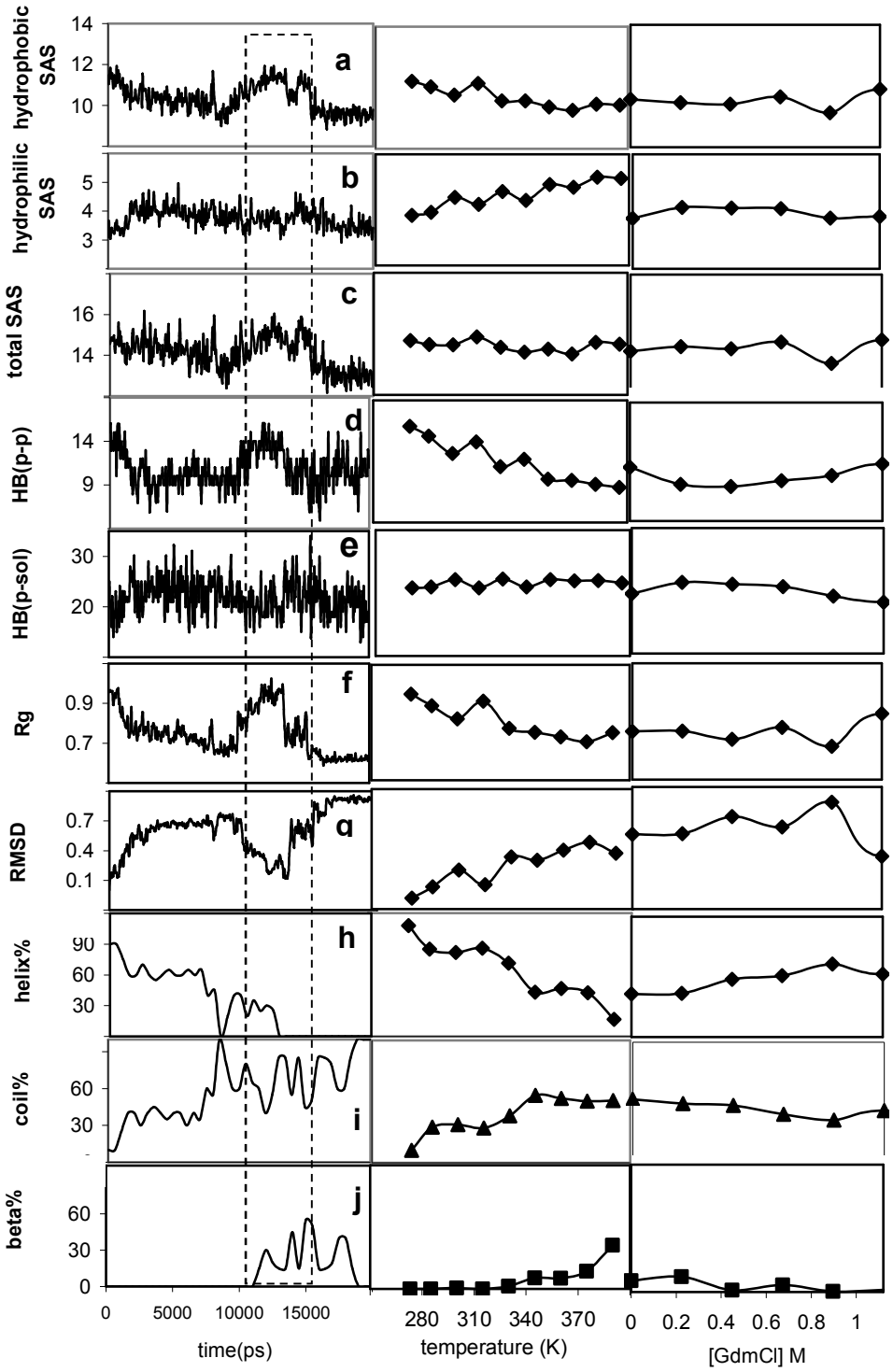

Fig. 2. Variation of structural parameters *vs*. time (left column), temperature (middle column), and guanidinium chloride concentration (right column). RMSD and R_g are in nm.

85% and 15%, respectively. The poly alanine underlies structural change in studied time duration and perfectly converted to the coil and beta at 5500 ps. The beta parallel is well shown at 6000 ps. After that, only the beta and coil exist in the systems which are converted to each other. These conversions fluctuate in the studied time range; whenever the beta increases, the coil decreases and *vice versa*.

The anti parallel beta structure is appeared at 14500 ps and 17000 ps and then polypeptide is converted to the coil after 19000 ps and resides in that form until the final time. Thus, the intermediate state can be related to beta formation and/or helix reformation after partial unfolding. Namely, when the polypeptide is partially unfolded, hydrophobic patches expose to the solvent and the probability of interaction of hydrophobic groups in different sites will be increased. Therefore, beta form appears and induces an order and stability to the polypeptide. This beta formation is accompanied with increasing the intra-peptide hydrogen bond, secondary structure and decreasing the surface area and RMSD. Calculated helix, coil and beta content by VADAR web server [52] are depicted in Figs. 3b-d. We applied consecutive kinetic mechanism for investigation of the conversion of helix to beta and coil. So, kinetic equations for conversion of helix to coil which pass through the beta form are as following [53]:

$$h \xrightarrow{k_1} b \xrightarrow{k_2} c$$
$$[h] = [h]_{\mathrm{o}}\, e^{-k_1 t} \tag{6a}$$

$$[b] = \frac{k_1[b]_{\mathrm{o}}}{k_2 - k_1}\left(e^{-k_1 t} - e^{-k_2 t}\right) \tag{6b}$$

$$[c] = [c]_{\mathrm{o}}\left[1 - \frac{k_2}{k_2 - k_1} e^{-k_1 t} + \frac{k_1}{k_2 - k_1} e^{-k_2 t}\right] \tag{6c}$$

Where, $[h]$, $[b]$ and $[c]$ are concentration in percent for helix, beta and coil, respectively. By fitting these equations to calculated $[h]$, $[b]$ and $[c]$ by means of Origin 5.0 software, the k_1 and k_2 values in different concentration of GdmCl can be obtained (solid line in Figs. 3b-d).

Variations of k_1 and k_2 *vs*. concentration of guanidine are depicted in Fig. 3e. The curves are similar to a bell. This might be related to the presence of intermediates and/or transition states, because the system is more complicated than two-state model. In the present work, we concern with three-state model. In this case, helix was converted to beta and coil. Beta conformation was appeared in the specific condition. Since beta formation dose not present in all temperatures, we couldn't perform kinetic analysis in all conditions. Therefore, we can estimate only activation energy for helix to product conversion that is naturally the first order.

$$h \xrightarrow{k} \text{product}$$
$$h = h_o e^{-kt} \tag{7}$$

The rate constant (k) obtained by fitting the above equation to helix percent in different times. By running this process for other conditions, especially higher temperatures, the k values are obtained. It is remembered that at higher temperature fitting error is less than that in lower one. Using Arehnius equation (Eq. (8)), the activation energy (E_{a}) is obtained from the slope of $\ln k$ *vs*. $1/T$ (Fig. 3f).

$$k = A e^{-E_a / RT}$$
$$\ln k = \ln A - \frac{E_a}{RT} \tag{8}$$

Then, the E_{a} is plotted *vs*. guanidine concentration. Fig. 3g shows that E_{a} increases with guanidine concentration. Thus, it seems that guanidine at low concentration decreases the rate of helix to coil transition and stabilizes the helix conformation.

It has been proved that guanidine denatures the macromolecule by two ways. One is related to direct effect on the macromolecule which is due to direct hydrogen bond, hydrophobic and electrostatic interaction with it, another way is related to the effect of this reagent on the solvent distribution. In comparison with osmolytes, GdmCl at higher concentration decreases protein hydration shell, while the osmolytes (polyols) which are used as stabilizer of proteins inversely increases it. Guanidine at high concentration has lower hydration tendency, moves toward protein and interacts with it, while the osmolystes do not. Osmolytes increase hydration layer of protein and move away from it as well as aggregate far from protein. Namely, the destabilizing denaturants are intruded near the protein

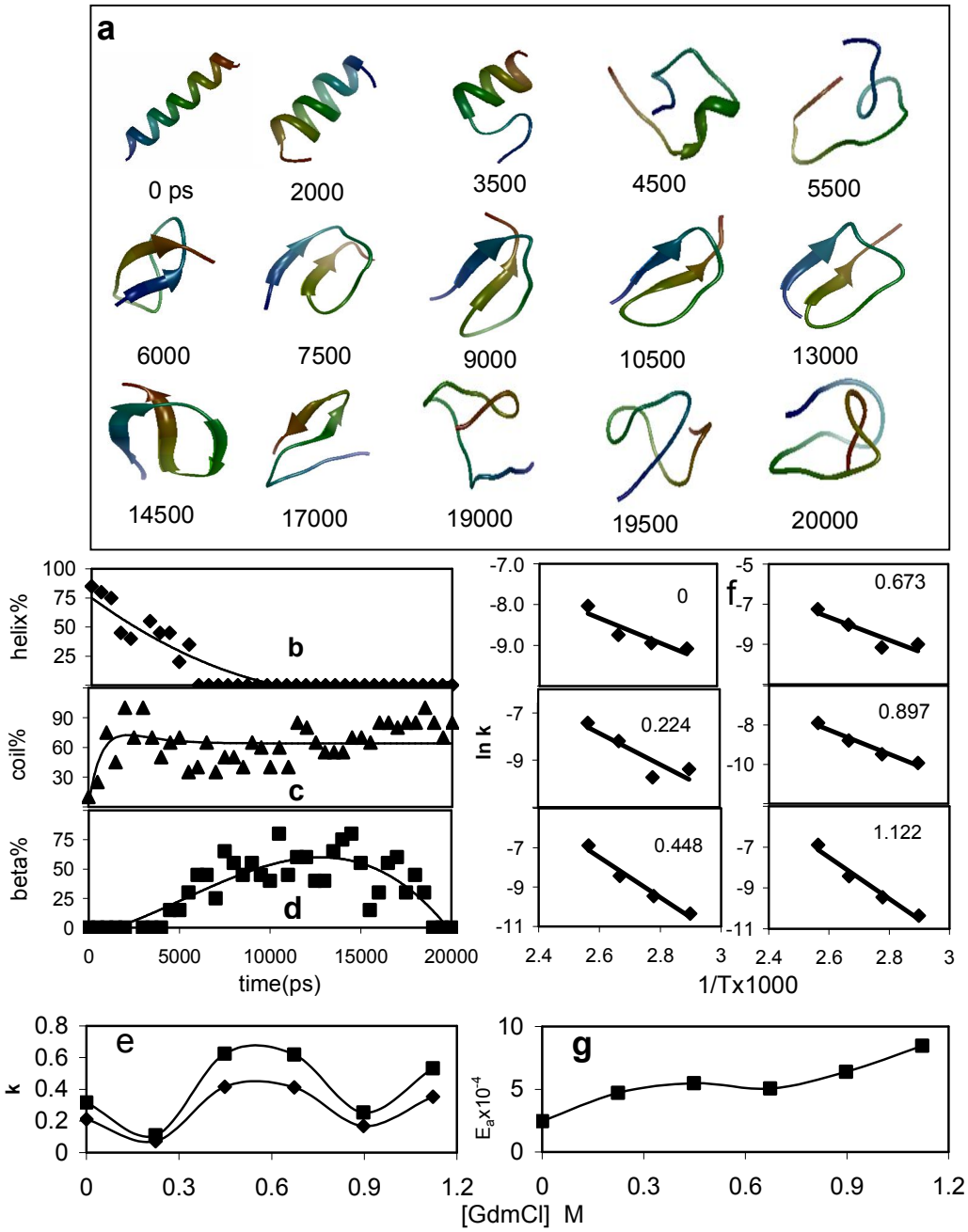

Fig. 3. (a) Time evolution for polyalanine structure during 20 ns molecular dynamics simulation and (b) helix (c) coil (d) beta percents calculated by VADAR (scatter data points) derived by fitting of equation (6) to calculated data (solid line) (e) Variation of rate constant for the first (k_1) and second step (k_2) related to helix to coil conversion obtained from equation (6) (f) variation of ln$k$ *vs*. inverse of temperature in different concentration of guanidine and (g) variation of activation energy derived from equation (8) against guanidinium chloride concentration.

and cause exclusion of water, while stabilizing agents are excluded from protein and cause water to migrate near the protein. So, the motion of all denaturant, solvent molecules and other ions are monitored in the vicinity and far from protein. To this purpose, the relative local distribution of water and guanidine molecules was characterized from MD trajectories, according to the RDF of the water and ligand around the peptide backbone atoms (Eq. (2)).

Figure 4 represents variations of solvent and guanidine distribution (RDF) around protein and guanidine ions.

Figure 4a shows RDF for water environ polyalanine in different concentration of GdmCl. The inset of figure and expanded parts (part b and c) depict the RDF at 0.3 nm. It increases up to 0.672 M guanidine, then decreases at 0.896 and 1.122. It means that GdmCl at low concentration increases the water around the protein and decreases it at higher concentration. On the other hand, trend of RDF at higher distance is inverse to lower distance. So, at low concentration (less than 0.896 M) guanidine behaves similar to osmolyte (*e.g.* trehalose) [5] while at higher concentration works same as urea and other denaturants.

Figure 4d represents the RDF for Gdm ion around protein. It is decreased with increasing ion concentration at near and far from protein. It has to be noted that bar lines in the Figs. 4d-h do not have labels due to limitation in space. Bar lines in Figs. 4d-h from left to right correspond to 0.224, 0.448, 0.672, 0.896 and 1.122 M guanidinium chloride. In order to clarify this phenomena we applied preferential hydration and exclusion concept. It is commonly considered as the reason for the protein stabilizing effect of protecting osmolytes. The mechanism indicates that water molecules in the hydration shell around the proteins increase because osmolyte molecules are excluded from the protein/solvent surface, thus inducing thermodynamic stabilization. Here, the preferential hydration of peptide in guanidine solutions can be investigated by analyzing water and guanidine distributions. Figure 4d shows RDF protein-guanidine at different guanidine concentrations. It is obvious that, within a distance of about 0.3 nm from the closest backbone atoms of polyalanine, the peptides become more and more preferentially hydrated when increasing guanidine concentration. By contrast to the preferential hydration on the peptides, at higher distance, there is a significant water depletion that results from the presence of many guanidine molecules. It can thus be concluded that there is a thin hydration shell on the surface of the peptides in guanidine solutions at low concentration. That is, guanidine molecules do not expel water molecules on the surface of the peptides; instead, water molecules are enriched as the guanidine concentration increases. These observations are also consistent with the experimental observation that osmolytes in aqueous solutions are totally excluded from the first hydration shell of protein [22].

Figure 4e shows that increasing the GmCl concentration increase the protein choloride interactions at short range but decreases at long range. It means that the chloride ion tends to move toward protein. Figure 4f shows RDF of water around ligand (Gdm). It is decreased in all concentration ranges. Figures 4d and 4f both show that guanidinium ion prefers to be far away from protein and become more solvated with increasing guanidine concentration. Figure 4g shows RDF guanidine-guanidine (Gdm-Gdm) which is decreased in the near and is increased at far distance from each other. RDF guanidinium ion also decreases in the near of protein, because guanidine tends to be aggregated far from polypeptide similar to osmolytes. Figure 4h shows distribution of chloride ions (RDF) around Gdm. This parameter decreases so that we can see chloride ion has moved to near the peptide.

On the other hand, unfolding of many proteins is accompanied by a large increase in C_p implying that the unfolding entropy and enthalpy depend strongly on temperature. Changes in C_p associated with protein unfolding come almost entirely from changes in hydration heat capacity due to exposing (solvation) of polar and nonpolar groups. Nonpolar solutes cause a concerted decrease in the average length and angle of the water-water hydrogen bonds in the first hydration shell, while polar and ionic solutes have the opposite effect. This is due to changes in the amounts, relative to bulk water, of two populations of hydrogen bonds: one with shorter and more linear bonds and the other with longer and more bent bonds [54].

Figure 5 shows helix, coil, beta percents as well as heat capacity of polyalanine at different temperatures in the absence and presence of 0.876 M and 1.122 M guanidine ions. In the absence of guanidine, helix% decreases while beta% and coil% increase due to increasing the temperature.

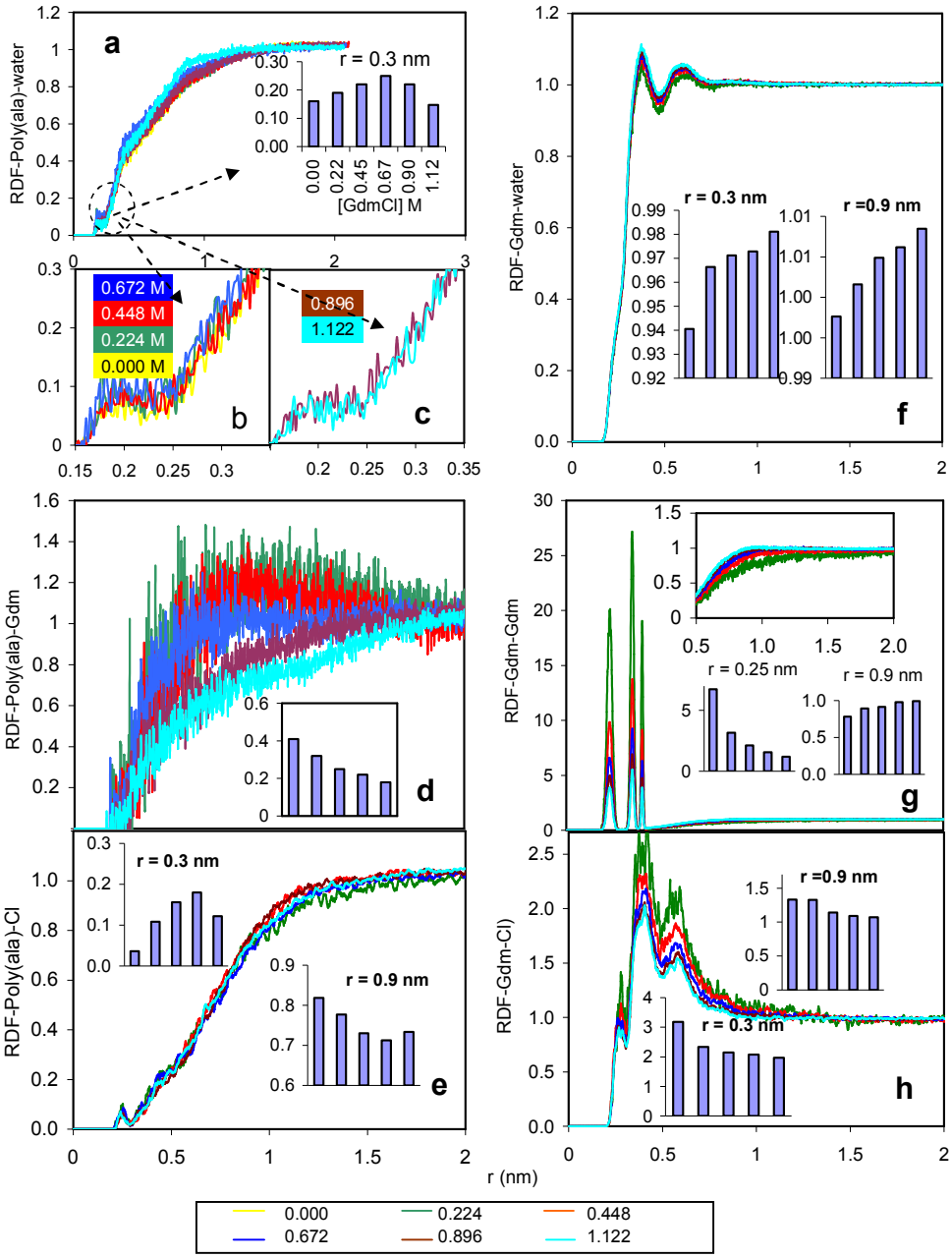

Fig. 4. Radial distribution function (RDF) for (a) water around center of mass polyalanine in the absence (yellow), and presence of 0.224 M (green), 0.448 M (red), 0.672 M (blue), 0.896 M (brown) 1.122 M (turquoise) of guanidinum chloride (b) expansion of part (a) for low concentration (c) expansion of part (a) for higher concentration of guanidinum chloride. RDF guanidinium (d) around polyalanine and RDF chloride ions (e) around polyalanine. RDF of water molecules (f), guanidinum (g) and chloride ions (h) environ guanidinum ion. Horizontal axes in bar lines curves represents the [GdmCl] in molar same as part (a). Bar line curves inset of figure 3 (except part a) from left to right are related to 0.224 M, 0.448 M, 0.672 M, 0.896 M and 1.122 M guanidinium chloride.

When the beta dose not exists, variation of helix and coil are perfectly inversed to each other. On the other hand, by appearance of the beta at higher temperatures, the previous order is not established, because sum of helix, coil and beta have to be equal to 100%. In addition, there are two minima or maxima in the helix and coil% curves. The first peak is related to the conversion of helix to partially unfolded (beta and/or reformed helix) and the second peak related to conversion of partially unfolded to totally coil structure. Figures 5b,c show helix, coil and beta percents in the presence of 0.673 and 1.122 M guanidine ion. Comparing with part (a), it is concluded that increasing the concentration causes peaks to move to the right.

Figures 5d-f show the C_p values versus temperature at three concentrations of guanidine. The shape of curves are approximately similar to differential scanning calorimetry (DSC) thermograms. DSC is usually used to investigate the thermal stability of macromolecules [10]. In addition, related helix%, coil% and beta% are plotted in the same concentrations. Figure 4a shows a peak at 300 K and another small peak at the 360 K. They are two T_ms for polypeptide. The first T_m belongs to the conversion of helix to beta and second concerns to the conversion of beta to unfolded coil state. It has been reported that the T_m of polypeptides is observed in the room temperature interval [55]. Comparison of C_p and helix shows that denaturation is accompanied with increasing C_p and decreasing helix (dashed rectangle in the Figure 5) *i.e.* trend of C_p is reverse of helix and is in direct to coil as well as beta form.

Figures 5b and c correspond to similar curve in the

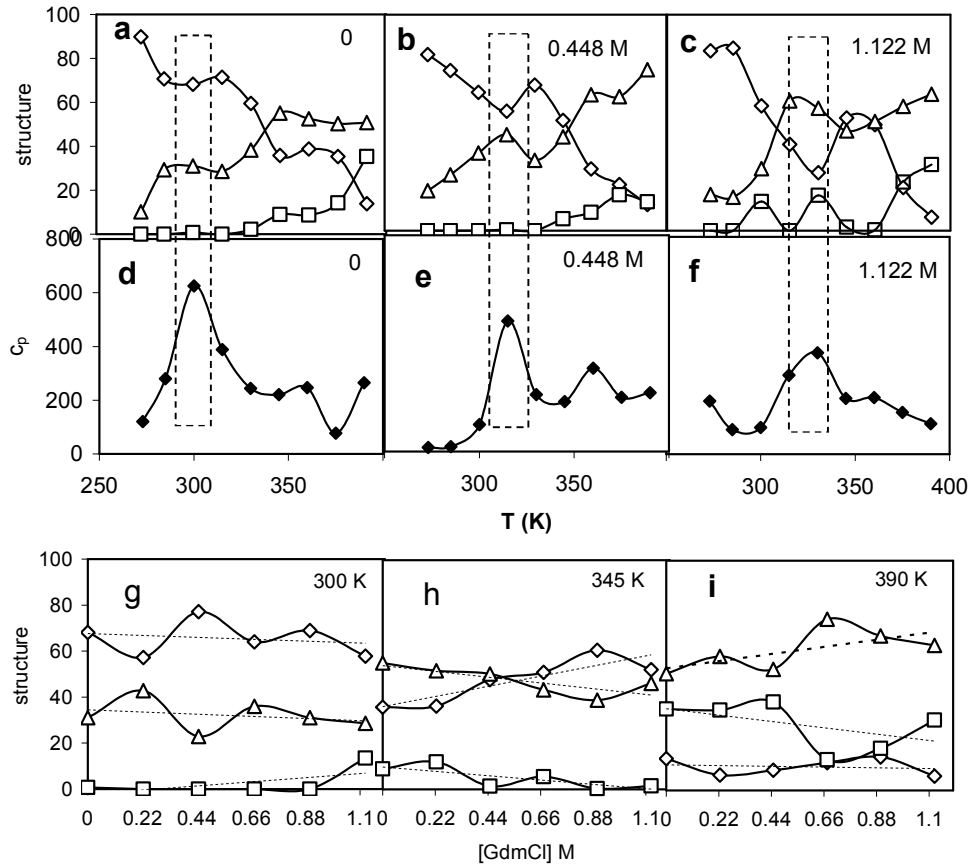

Fig. 5. Helix (◇), coil (△), beta (□) contents in percent and heat capacity (◆) *vs*. temperature at three concentrations of GdmCl (a-f). Helix, coil, beta percents *vs*. guanidinium chloride concentration at three temperatures (g-i).

presence of 0.673 and 1.122 M GdmCl, respectively. Namely, trend of C_p variation has inverse correlation with helix and direct correlation with coil and beta. The first T_m of polypeptide is 300 K in the absence of GdmCl, while it is 315 and 330 K in the presence of 0.673 and 1.122 M GdmCl, respectively. Therefore, it seems that ligand increases the T_m and protein stability. To support this idea, the variation of helix, coil and beta were plotted in different concentration of guanidine at 300, 345 and 390 K.

Trend of coil is the inverse of helix, while beta structure only appears at 0.896 to 1.122 M guanidine. At 345 K, total coil is less than corresponding value at 300 K and decreases with guanidine and also is in inverse of helix and coil. On the other hand, total beta is higher than 300 K and the trend is decreasing. At 390 K, total amount of coil and beta is higher and the amount of helix is lower compared to that of in lower temperatures.

CONCLUSIONS

Guadindium chloride is the most popular denaturant that unfolds protein at high concentration. However, there are a number of evidences that it stabilizes the macromolecues at low concentration as the same as osmolystes. It increases activation energy and midpoint of transition temperature (T_m) for helix to coil phase transition. On the other hand, it increases the hydration shell of polypeptide regarding to radial distribution function results. In addition, it displaces and is expelled from surface of polypeptide and decreases the beta formation and prohibits the interamolecular interaction. Thus, it can be used as reducing factor for aggregation and the related diseases. This behavior has been also observed in the osmolyte case.

ACKNOWLEDGEMENTS

The financial support of Damghan University, specially research council and IT center are gratefully acknowledged.

REFERENCES

[1] B. Leitge, A. Kerényi, F. Bogár, G. Paragi, B. Penke, G. Rákhely, Mol. Model. 13 (2007) 1141.
[2] S. Yang, M. Cho, J. Phys. Chem. B. 111 (2007) 605.
[3] R.W. Carrell, D.A. Lomas, Lancet 350 (1997) 134.
[4] L.J. Simons, B.W. Caprathe, M. Callahan, J.M. Graham, T. Kimura, Y. Lai, H. Levine, A.W. Lipinski, A.T. Sakkab, Y. Tasaki, L.C. Walker, T. Yasunaga, Y. Ye,. N. Zhuang, C.E. Augelli-Szafran, Bioorg. Med.Chem. Lett. 19 (2009) 654.
[5] F.-F. Liu, L. Ji, X.-Y. Dong, Y. Sun, J. Phys. Chem. B 113 (2009) 11320.
[6] D. Ajloo, A.A. Saboury, N. Haghi-Asli, G. Ataei-Jafarai, A.A. Moosavi-Movahedi, , M. Ahmadi, K. Mahnam, S. Namaki, J. Enzym. Inhib. Med. Chem. 22 (2007) 395.
[7] A.A. Moosavi-Movahedi, S. Safarian, G.H. Hakimelahi, G. Ataei, D. Ajloo, S. Paojehpour, S. Riahi, M.F. Mousavi, S. Mardanyan, N. Soltani, A. Khalafi-Nezhad, H. Sharghi, H. Moghadamnia, A.A. Saboury, Nucleos. Nucleot. Nucl. 23 (2004) 613.
[8] D. Ajloo, A.A. Moosavi-Movahedi, G.H. Hakimelahi, A.A. Saboury, H. Gharibi, Colloids, Surfaces B, Biointerfaces 26 (2002) 185.
[9] A.K. Bordbar, A. Nasehzadeh, D. Ajloo, K. Omidiyan, H. Naghibi, M. Mehrabi, H. Khajehpour, M. Rezaei-Tavirani, A.A. Moosavi-Movahedi, Bull. Korean Chem. Soc. 23 (2002) 1073.
[10] M. Rezaei-Tavirani, A.A. Moosavi-Movahedi, S.Z. Moosavi-Nejad, J. Chamani, D. Ajloo, Thermochim. Acta 408 (2003) 9.
[11] P. Dasmeh, D. J. Searles, D. Ajloo, Denis J. Evans, and Stephen R. Williams, J. Chem. Phys. 131 (2009) 214503.
[12] X. Wu, G. Narsimhan, Molecular Simulation 35 (2009) 974.
[13] K. Bisetty, H.G. Kruger, J. J. Perez, Molecular Simulation 33 (2007) 1105.
[14] C. Niedermeier, K. Schulten, Molecular Simulation 8 (1992) 361.
[15] D. Ajloo, E. Taghizadeh, A.A. Saboury, E. Bazyari, K. Mahnam, Int. J. Biol. Macromol. 43 (2008) 151.
[16] I.A. Solov'yov, A.V. Yakubovich, A.V. Solov'yov, W. Greiner, Phys. Rev. E 51912 (2007) 1.
[17] I.K. Lednev, A.S. Karnoup, M.C. Sparrow, S.A. Asher, J. Am. Chem. Soc. 123 (2001) 2388.
[18] S. Williams, R.G. Thimothy P. Causgrove, K.S. Fang, R.H. Callender, W.H. Woodruff, R.B. Dyer,

Biochemistry 35 (1996) 691.
[19] S. Yang, M. Cho, J. Phys. Chem. B 111 (2007) 605.
[20] A.V. Yakubovich, I.A. Solov'yov, A.V. Solov'yova, W. Greiner Eur. Phys. J. D 51 (2009) 25.
[21] O.V. de Oliveira, A.F. de Moura, L.C.G. Freitas, J. Mol. Struc.-Theochem. 808 (2007) 93.
[22] T. Arakawa, R. Bhat, S.N. Biochemistry 29 (1990) 1914.
[23] Y. Kita, T. Arakawa, T.Y. Lin, S.N. Timasheff, Biochemistry 33 (1994) 15178.
[24] J. Fitter, S. Haber-Pohlmeier, Biochemistry 43 (2004) 9589.
[25] L. Huaa, R. Zhoua, D. Thirumalaic, B. J. Bernea, Proc. Natl. Acad. Sci. USA 105 (2008) 16928.
[26] T.P.E. Mason, G.W. Neilson, C.E. Dempsey, A.C. Barnes, J.M. Cruickshank, Proc. Natl. Acad. Sci. 100 (2003) 4557.
[27] R.L. Baldwin, Biophys. J. 71 (1996) 2056.
[28] K.D. Collins, Proc. Natl. Acad. Sci. USA 92 (1995) 5553.
[29] Q. Zou, S.M. Habermann-Rottingaus, K.P. Murphy, Proteins 31 (1998) 107.
[30] A. Wang, D.W. Bolen, Biochemistry 36 (1997) 9101.
[31] J. Chugh, S. and R.V. Hosour, Arch. Biochem. Biophys. 481 (2009) 169.
[32] A. Zarrine-Afsar, A. Ittermaier, L. Kay, A. Davidson, Protein Sci. 15 (2006) 162.
[33] J.A. Schellman, Biophys. Chem. 96 (2002) 91.
[34] K.D. Collins, Methods 34 (2004) 300.
[35] L.M. Mayr, F.X. Schmid, Biochemistry 32 (1993) 7994.
[36] O.D. Monera, C.M. Kay, R.S. Hodges, Protein Sci. 3 (1994) 1984.
[37] G.I. Makhatadze, M.M. Lopez, J.M. Richardson, S.T. Thomas, Protein Sci. 7 (1998) 689.
[38] A.K. Bhuyan, Biochemistry 41 (2002) 13386.
[39] A.W. Schuttelkopf, D.M. van Aalten, Acta Crystallogr. D 60 (2004) 1355.
[40] W. Weber, P.H. Hunenberger, J.A. McCammon, J. Phys. Chem. B 104 (2000) 3668.
[41] R.E. Bruccoleri, M. Karplus, Biopolymers 29 (1990) 1847.
[42] J.L. Rosas-Trigueros, J. Correa-Basurto, C.G. Benítez-Cardoza, A. Protein Sci. 12 (2011) 2035.
[43] D. Van Der Spoel, E. Lindahl, B. Hess, G. Groenhof, A.E. Mark, H.J. Berendsen, Comput. Chem. 26 (2005) 1701.
[44] W.F. Van Gunsteren, S.R. Billeter, A.A Eising, P.H. Hunenberger, P. Kruger, A.E. Mark, W.R.P. Scott, I.G. Tironi, Biomolecular Simulation: The GROMOS96 Manual and User Guide, Zürich, Switzerland, Groningen, Holland, 1996.
[45] H.J.C. Berendsen, J.P.M. Postma, W.F. van Gunsteren, J. Hermans, in: B. Pullman (Ed.), Interaction Models for Water in Relation to Protein Hydration. In Intermolecular Forces, Reidel: Dordecht, Holland, 1981, pp. 331-342.
[46] L. Verlet, Computer Phys. Rev. 159 (1967) 98.
[47] T. Darden, D. York, L. Pedersen, J. Chem. Phys. 98 (1993) 10089.
[48] B. Hess, H. Bekker, H.J.C. Berendsen, J.G.E.M. Fraaije, Comput. Chem. 18 (1997) 1463.
[49] S. Nosé, Mol. Phys. 52 (1984) 255.
[50] W.G. Hoover, Phys. Rev. A 31 (1985) 1695.
[51] M. Parrinello, A. Rahman, Phys. Rev. Lett. 45 (1980) 1196.
[52] L. Willard, A. Ranjan, H. Zhang, H. Monzavi, R.F. Boyko, B.D. Sykes, D.S. Wishart, Nucleic Acids Res. 31 (2003) 3316.
[53] J.I. Steinfeld, J.S. Francisco, W.L. Hase. Chemical Kinetics and Dynamics Printice-Hall International Edition, New Jersey, 1983.
[54] A.V. Persikov, J.A.M. Ramshaw, B. Brodsky, J. Biol. Chem. 280 (2005) 19343.
[55] K.A. Sharp, B. Madan, J. Phys. Chem. B 101 (1997) 4343.